Journal of Cleaner Production 423 (2023) 138728

Contents lists available at ScienceDirect

Journal of Cleaner Production

journal homepage: www.elsevier.com/locate/jclepro

Nitrogen doped carbon dots as a photocatalyst based on biomass. A life cycle assessment

Gabriela Rodríguez-Carballo [a], Ramón Moreno-Tost [a,**], Sónia Fernandes [b], Joaquim C. G. Esteves da Silva [b,c], Luís Pinto da Silva [b,c], Eulogio Castro Galiano [d], Manuel Algarra [e,*]

[a] Universidad de Málaga, Departamento de Química Inorgánica, Cristalografía y Mineralogía, Facultad de Ciencias, Campus de Teatinos, (Unidad Asociada al ICP-CSIC), 29071, Málaga, Spain
[b] Chemistry Research Unit (CIQUP), Institute of Molecular Sciences (IMS), Department of Geosciences, Environment and Territorial Planning, Faculty of Sciences, University of Porto, Rua do Campo Alegre s/n, 4169-007, Porto, Portugal
[c] LACOMEPHI, GreenUPorto, Department of Geosciences, Environment and Territorial Planning, Faculty of Sciences, University of Porto, Rua do Campo Alegre s/n, 4169-007, Porto, Portugal
[d] Department of Chemical, Environmental and Materials Engineering, Centre for Advanced Studies in Earth Sciences, Energy and Environment (CEACTEMA), University of Jaén, Jaén, 23071, Spain
[e] INAMAT^2-Institute for Advanced Materials and Mathematics, Department of Sciences, Public University of Navarre, Campus de Arrosadía, 31006, Pamplona, Spain

ARTICLE INFO

Handling Editor: Jin-Kuk Kim

Keywords:
Carbon dots
Xylose
Acid catalyst
Biomass
Nanoparticles
Hydrothermal synthesis
Photoluminescence
Photocatalysis
Life cycle assessment

ABSTRACT

The effectiveness of various transition metal phosphate-based acid catalysts, including vanadium and niobium, in the hydrothermal synthesis of carbon dots (CDs), has been assessed. Two sources of carbohydrates were employed for this: commercial xylose and liquor of xylose produced by processing olive pits. Catalysts were identified using the NH_3-TPD, DTA/TG, XRD, and XPS techniques. The reaction was conducted for 4 h at a temperature of 180 °C. The existence of such nanoparticles, regardless of the carbohydrate source, was confirmed by an analysis of the features and characteristics of CDs nanoparticles. N-doped CDs with increased fluorescence were also created at the same time using a similar hydrothermal technique, and their photocatalytic activity was investigated. A Life Cycle Assessment (LCA) was conducted for both syntheses with the goal of comparing the environmental effects of the synthesis from commercial xylose to the synthesis from biomass. It was revealed that, although energy is the primary driver of both synthesis pathways' effect categories, the fundamental variations that seem to determine their relative sustainability are connected to the nature of the carbon precursor. Regarding the latter, it is determined that electricity has the greatest environmental impact.

1. Introduction

CDs are recently discovered nanoparticles and present unique properties. Each nanoparticle consists of a graphitic lattice core covered by a functionalized surface composed by several polar functional groups attached (Hola et al., 2014; Zhu et al., 2020), making these nanoparticles extremely soluble in aqueous solutions. CDs can be obtained via two main synthetic approaches: from small molecules aggregation, the bottom-up route, or from larger carbon structures such as graphite, graphene or nanotubes, the top-down route (Tajik et al., 2020).

A current tendency for obtaining CDs is the pursuit of a synthesis method that fulfils the requirements of green chemistry but keeps production costs low. Therefore, CDs obtained from green precursors coming from biomass is an emergent research topic (Rodriguez-Padrón et al., 2018; Algarra et al., 2019; Sim et al., 2019; Crista et al., 2020; Y. Wu et al., 2021; El-Shabasy et al., 2021; Kurian and Paul, 2021). The most frequent and best-known method for CDs production is hydrothermal or solvothermal method (Sim et al., 2019; Zhu et al., 2020; Kurian and Paul, 2021; Yin et al., 2021). This method requires acidic conditions commonly achieved using mineral acids such as HCl, nonetheless, the hydrothermal method is compatible with heterogeneous catalysis, providing that the selected catalysts are in the acid environment to promote successive dehydration, condensation and superior aggregation processes leading to the generation of CDs (Xiong et al., 2021; Singh et al., 2023).

Due to admitting functionalization on their surface, CDs exhibit

* Corresponding author.
** Corresponding author.
E-mail addresses: rmtost@uma.es (R. Moreno-Tost), manuel.algarra@unavarra.es (M. Algarra).

https://doi.org/10.1016/j.jclepro.2023.138728
Received 22 May 2023; Received in revised form 1 September 2023; Accepted 5 September 2023
Available online 10 September 2023

photoinduced electronic transference, fluorescence, and up-conversion photoluminescence (Sim et al., 2019). CDs have raised increasing attention for their undemanding synthesis procedure combined with the fact that they have been proved to be non-toxic and can be modified to reach satisfactory quantum yield values (Kaur et al., 2021). CDs photoluminescence presents variation with size, showing a strong dependency on the energy gap between valence and conduction bands, that corresponds to the HOMO-LUMO (the highest occupied molecular orbital and lowest unoccupied molecular orbital, respectively) gap, as size increases, gap decreases (Macairan et al., 2022). As CDs are functionalized by a great variety of groups, these nanoparticles exhibit surface state photoluminescence, considering that the functional groups on their surface have multiple energy levels that can interact and result in emissive traps, thus dominating the emission. The surface state is a synergetic contribution of all groups conforming the surface of the CDs that hybridize with the outer graphitic core. This interaction between the core and the functional groups should not be mistaken as molecular state. Molecule state refers to the photoluminescence expected when an organic fluorophore is attached to the surface of the CDs. These CDs show exceedingly high quantum yields and strong photoluminescence, whereas when surface state is the predominant effect causing emission, CDs tend to exhibit much lower photoluminescence, but higher photostability (Zhu et al., 2015).

Several materials have been proposed as semiconductors to carry out photochemical reactions for a wide variety of purposes. The materials put to the test have mostly been metal-based. Currently, the novel trend is the utilization of metal nanoparticles, such as quantum dots (QDs). Despite its great performance in vacancy generation and electron movement, their production method is still costly and time consuming. Furthermore, metal-based photocatalysts will lead to unavoidable metal leakage in time (Zhu et al., 2022). Because of their photoluminescence and electron transfer properties, CDs can work as electron mediators, photosensitizers, as well as photocatalysts by themselves (Khan et al., 2022). It has been proved that CDs when photo excited are outstandingly good electron donors and electron acceptors, since either electron acceptors or electron donors are able to quench the photoluminescence emitted by CDs effectively (Dhamodharan et al., 2022). CDs provide an environmentally friendly alternative to their metal analogues. A variety of techniques can be used over virgin carbon nanoparticles to achieve an improvement in its photocatalytic and emissive features, such as surface functionalization and doping. Using CDs as catalysts in photoreactions bring some advantages along. CDs exceed by far other conventional catalyst such as TiO_2, ZnO and CdS in terms of solubility in aqueous solutions, chemo-stability, and toxicity. Surface of CDs can be modified to tune the absorbance of CDs and up-converted fluorescence that can help increasing the effectiveness of the absorption of sunlight of semiconductors from infrared to visible regions of the spectrum (Jung et al., 2022).

CDs are exceedingly versatile nanoparticles that find application in diverse fields such as bioimaging (Hola et al., 2014), biological (Wang et al., 2021), chemical sensors (Campos et al., 2016; Li et al., 2017, 2018), photocatalysis (Bramhaiah et al., 2021; Q. Wu et al., 2021), drug delivery (Nocito et al., 2021), next generation light emitting devices (Perikala and Bhardwaj, 2021), and immunoassays (Sharma et al., 2021). They are usually prepared from biomass and exhibit considerably low quantum yield (<10%). As a result, doping has emerged as a promising strategy to improve CDs quantum yields, reaching values near 60% (Liao, Cheng, and Zhou, 2016). Nitrogen is a frequent dopant of CDs, as N doped CDs have abundant surface-state defects (Zheng et al., 2021). Up until now, three aromatic N species have been identified to always appear in CDs framework: pyridinic, pyrrolic and graphitic nitrogen (Hao et al., 2021). CDs provide an environmentally friendly alternative to their metallic analogues. To the best of our knowledge, almost all catalysts assayed in CDs heterogeneous-catalysed production are metal oxides. Since vanadium phosphate (VPO) catalysts and their Nb analogues are known for being capable of promoting carbohydrates further dehydration into platform chemicals, such as 5-hydroxymethylfurfural (HMF) and furfural, they were selected as catalysts for a novel CDs production method, as one of the main steps of CDs synthesis involves the dehydration and further condensation and aggregation of the precursors (Xiong et al., 2021; Yin et al., 2021). Hydrothermal method also enables the simultaneous heteroatom doping and generation of CDs via a one-pot synthesis with a dopant (Sim et al., 2019; Zheng et al., 2021).

One of the most appropriated approaches to understand the associated environmental impacts of given products/processes is life cycle assessment (LCA). This tool can characterize the potential environmental impacts of a given system during its entire life cycle. More specifically, this can be achieved through the identification and quantification of potential impacts from raw materials extraction until to end-of-life, including the manufacturing/use stage (Ramos, Texeira and Roubia, 2018; Sendão et al., 2020; Fernandez, Esteves da Silva and Pinto da Silva 2021). It is noteworthy that an LCA study can provide multiple impact categories for evaluation of target products/systems (Marras et al., 2015). LCA approaches has already been used to evaluate the environmental impacts associated with different systems such as wind farms (Bi et al., 2021), dairy products [Kumar, et al., 2021), ceramic industry (Monteiro, Cruz, and Moura, 2022) and different types of engineered nanomaterials (Crista et al., 2020; Christé, Esteves da Silva and Pinto da Silva, 2020). In fact, members of this team have been focused on the evaluation, through LCA studies, of the environmental sustainability of fabricating CDs (Crista, Esteves da Silva and Pinto da Silva 2020; Sendão et al., 2020; Christé, Esteves da Silva and Pinto da Silva, 2020; Fernandez, Esteves da Silva and Pinto da Silva 2021; Fernandez, Esteves da Silva and Pinto da Silva 2021).

In this research, we successfully produced CDs utilizing a hydrothermal technique with commercial xylose and olive pit biomass as carbonous feedstock, as well as $VOPO_4$ and $NbOPO_4$ as catalysts. Then, the produced CDs were examined using TEM, XPS, and a confocal photoluminescence microscope to characterize them. The environmental sustainability of the synthetic CDs made using commercial xylose and olive pit biomass as carbonous feedstock was assessed using life cycle assessment (LCA). The resulting CDs were then successfully used in the photocatalyst-based degradation of methyl orange.

2. Materials methods

2.1. Materials

Vanadium (V) oxide, V_2O_5 (Aldrich Chemie, >99,6%); niobium oxalate monooxalate adduct, $Nb(HC_2O_4)_5$ (ABCR); Xylose (Millipore, >98%); orthophosphoric acid, H_3PO_4 (Panreac, >85%); ammonium chloride, NH_4Cl (Sigma-Aldrich, >99,5%); nitric acid, HNO_3 (VWR, >65%).

2.2. Synthesis

2.2.1. Catalyst

2.2.1.1. Preparation of the catalyst. Both $VOPO_4$ and $NbPO_4$ catalysts were prepared according to previously described methods (Luo et al., 2015; Zhu et al., 2020). Briefly, $VOPO_4$ was prepared from 1.93 g of V_2O_5 stirred magnetically with H_3PO_4 (10.5 mL), V:P molar ratio of 1; H_2O (22 mL) and concentrated HNO_3 (2 mL) and kept under reflux conditions for 2 h at 105 °C, then the yellow solid was filtrated and left to dry in the stove overnight at 60 °C. $NbOPO_4$ was obtained following a similar method, starting from 2.78 g of $Nb(HC_2O_4)_5$, stirred magnetically with 20 mL of deionized water and 2.2 mL of phosphoric acid, being the Nb:P molar ratio of 1, at 115 °C for 48 h. The white solid was separated from the solution by centrifugation, and it was left to dry overnight at room conditions. Characterization based in XRD, Raman,

TPD is found in Supplementary Information (S.I) Figures SI1-3.

2.2.2. Synthesis of carbon dots (CDs)

Two sources of xylose were selected for the CDs synthesis: commercial xylose and xylose contained in the liquor prepared from olive pits treatment (see below). The preparation of CDs (Scheme 1) from commercial xylose involved 50 mL of 0.75 M solution of xylose and 100 mg of catalyst $VOPO_4$ or $NbOPO_4$ that were added into a hydrothermal Teflon-lined steel reactor. After catalyst addition, the pH of the suspension was measured and varied from 2 to 3.5, depending on the catalyst. The reaction was kept at 180 °C and the reaction time was set at 4 h, respectively. The product obtained following the centrifugation and filtration of the reaction solution was a vibrant yellowish orange solution and when irradiated under UV light showed modest fluorescence. This solution was further purified to obtain a clean solution of CDs. In this regard, the yellowish orange solution of CDs underwent a treatment including three steps. First, the solution was centrifuged along with 10 mL of a pH 4.7 buffer solution (Afonso et al., 2021). Next, the solution was dialyzed *v*. H_2O (1 L). After 48 h of dialysis, a CDs pale yellow solution was obtained, and its photoluminescence was tested under UV lamp to ensure the dialysis was performed correctly. Finally, the dialysed solutions were treated with $N_{2,\ liq}$ (−196 °C) in constant stirring, when all solution was frozen, it was lyophilized in a Scanvac Coolsafe 110-4 Pro during 48 h. Synthesis of CDs from biomass liquor was essentially like that of commercial xylose. In Table 1 are shown the main characteristics of the liquor obtained from olive pits. The xylose-enriched liquor from olive pits was produced in an autoclave. Briefly, 1500 g of crushed olive pits were soaked with 1500 g of a 2% sulfuric acid solution and put into a crystal bottle inside the autoclave. Target temperature was set at 125 °C for 30 min once this temperature was attained (in the used device, heating time was approximately 20 min and cooling time also 20 min). After this time, solids and liquid fractions were separated by vacuum filtration.

The autoclave treatment resulted in a high dissolution of the hemicellulose fraction of olive pits, with xylose as the main sugar. Once the liquor was obtained, the CDs synthesis was carried out following the same procedure as it was mentioned before, the liquor was transferred along with 100 mg of catalysts into the hydrothermal reactor and pH was measured providing values from 1 to 1.3, substantially lower than with commercial xylose since biomass liquor was prepared from acid itself. Both temperature and reaction time were the same as with commercial xylose. Furthermore, the CDs was also submitted to the purification steps previously described.

2.2.3. CDs doping with N

CDs doped with nitrogen moieties (N-CDs) were synthesized via a one-step hydrothermal method as well. 100 mg of $VOPO_4$ or $NbOPO_4$ catalyst, 25 mL of 0.75 M xylose and NH_4Cl (5 g and 7.5 g) as dopants were added into a Teflon lined stainless steel reactor. pH was measured to ensure that acidic conditions were appropriate for the reaction to proceed, obtaining values from 2.3 to 2.5 for nitrogen solution.

Table 1
Composition of biomass liquor (g/L).

Sugars		Other compounds	
Glucose	4.19	Formic acid	1.10
Xylose	69.97	Acetic acid	17.58
Galactose	8.19	HMF	0.13
Mannose	0.404	Furfural	0.21
Arabinose	9.86		

2.3. Liquor aging

With the aim of studying the effect of further degradation of liquor in the obtention of biomass CDs, the liquor was left to age for different time periods: a day, a week, and two weeks. Aging the liquor did not worsen its characteristics and properties, that were measured by means of HPLC.

2.4. Characterization

Transmission Electron Microscopy (TEM) was performed in a FEI-Talos F200X equipped with FEG 200 kV electron gun, four STEM detectors and four FEG detector and Thermo Scientific-FEI Tecnai G2 20 Twin Transmission Electron Microscope equipped with LaB_6 filament, tomography software, cryo-transmission system and EDS/EDX (Energy Dispersive X-ray Spectroscopy) elemental analyzer used to carry out the superficial analysis of CDs. The optical properties of the CDs were evaluated by photoluminescence measurements using a LabRAM Odyssey PL microscope (Horiba). Zeta potential (ζ) was measured aiming an evaluation of the superficial electric charge of CDs nanoparticles Measurements were performed using a 4mWHeNe Laser Doppler Velocimetry laser working at a fixed wavelength of 633 nm via an automatized procedure in a Malvern Zetasizer Nano ZS. The superficial composition of the CDs was analyzed by XPS This analysis was conducted in a Physical Electronics PHI5700 spectrometer using monochromatic MgK_α radiation of 300 W, 15 kV and 1253.6 eV with a multichannel detector. Analysis zone comprised an area of 720 μm of diameter and constant pass energy mode was set at 29.35 eV. The spectrum obtained was processed using MultiPak *v*.9.3 software. The XPS analysis was carried out to the lyophilized samples. All values were referenced to adventitious carbon (C 1*s* at 284.8 eV). Functional groups were studied by means of FTIR using a Shimadzu FTIR-8300 infrared spectrophotometer for the case of CDs that were shaped into wafers along with KBr and irradiated under a 0.5 mW power IR-beam at a fixed

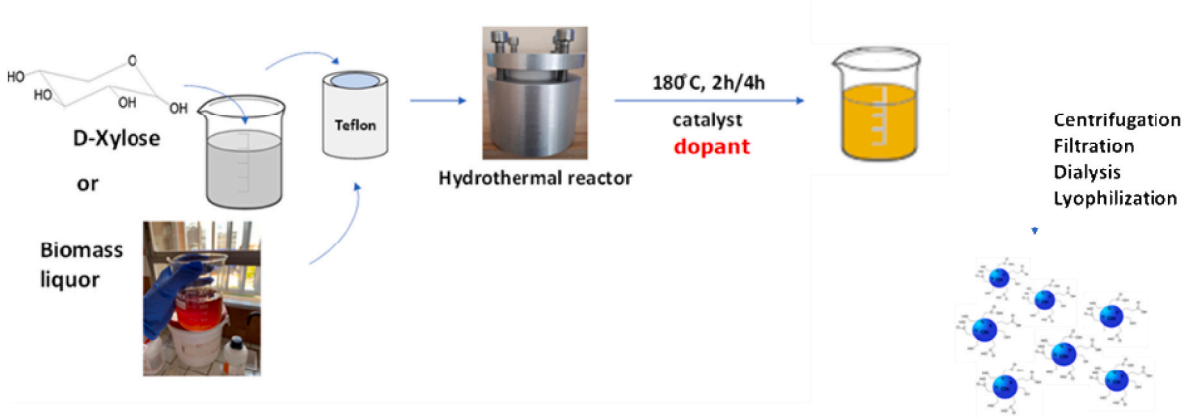

Scheme 1. Hydrothermal synthesis of CDs from commercial xylose and biomass liquor.

wavelength of 632.8 nm. Whereas N-CDs were also lyophilized but the solid was analyzed by means of FTIR-ATR using a Jasco Analytics 6800FV infrared spectrophotometer coupled with an ATR ProOne accesory. The remaining xylose in reaction samples was controlled using HPLC instrument (JASCO) equipped with an autoinjector (AS-2055) which injects 6 μL of the sample in a Phenomenex Rezex RCM-Monosaccharide Ca^{2+} (8%) (300 mm × 7.8 mm, 5 μm) column. The mobile phase (deionized and degassed water) was pumped by a quaternary gradient pump (PU-2089) at 0.4 mL/min flow rate to the column. The column is thermostatic at 70 °C.

2.5. Photocatalytic activity

N doped CDs (0.05 g) were added into 500 mL of 5 ppm methyl orange (MO) ethanol-water solution. Samples were irradiated by visible light inside photoreactor (Luzchem Model CCP-4V 220 V 50 Hz 3 A) with mechanical stirring and equipped with fourteen white visible lamps. Aliquots were taken after 5, 10, 20, 30, 60 and 80 min to study MO photodegradation. The photodegradation of MO was followed by Spectrophotometry UV (UV, 1800 SHIMADZU UV). Sample concentration was calculated by interpolation to the calibration curve obtained from standards measurements (2, 3, 4, 5 ppm and 0.2, 0.3, 0.4, 0.5 ppm) (Figure SI6). The total carbon and/or total nitrogen content of aqueous samples was analyzed by means of TOC Analyzer (Analytikjena multi-N/C 3100).

2.6. Life cycle assessment

This study consists in a cradle-to-gate LCA that intends to quantify and compare the potential environmental impacts associated with the synthesis of the two studied CDs (Scheme 2). More specifically, the present study is focused on the laboratory-scale synthesis of the target nanoparticles and considers the direct emissions from CDs production, as well as indirect impacts related with upstream resource extraction and energy generation. The environmental impacts were analyzed and compared by using a weight-based functional unit of 1 kg (kg). The environmental impacts related to the CDs syntheses were assessed based on inventory data from laboratory-scale synthesis procedures found in Ecoinvent® 3.5 database. Potential environmental impacts were assessed according to ReCiPe (2016) V1.03 endpoint method (Huijbregts et al., 2017) and the LCA study was performed using SimaPro 9.0.0.48 software. The environmental impacts under study were categorized in terms of Human Health, Ecosystems and Resources. Detail information about endpoint indicators is described in Supplementary Information.

2.6.1. Life cycle inventory data

The chemicals used as raw materials and the electricity used for the fabrication process constitutes the foreground system of the synthesis procedure. In this sense, the different processes, as well as the chemicals included in this study were modelled with the data present in the Ecoinvent® 3.5 database. As referred above, the electricity included was the required for the use of autoclave (power consumption of 3200 W and a vacuum pump with 180 W), centrifuge (power consumption of 500 W), heating and stirring plate (power consumption of 1000 W) and furnace (power consumption of 1800 W). For the xylose production it was considered the synthesis route described previously (Sharma et al., 2020). It is worth mentioning that for this LCA study it was not considered the catalysts used in the CDs production, since they are not consumed in these reactions. It should also be noted that olive pits in biomass liqueur production were also not considered in the inventory, as they are waste material that is generated because of the production of olive oil. Thus, in the framework of this study, we attributed the environmental impacts resulting from the production of olive pits to the olive oil industry and considered its use as precursor as the absence of the need to employ instead commercial precursors (Algarra et al., 2018). The used materials and electricity are reported in Table 2.

2.6.2. Sensitivity analysis

It was performed a sensitivity analysis by considering "What-if"

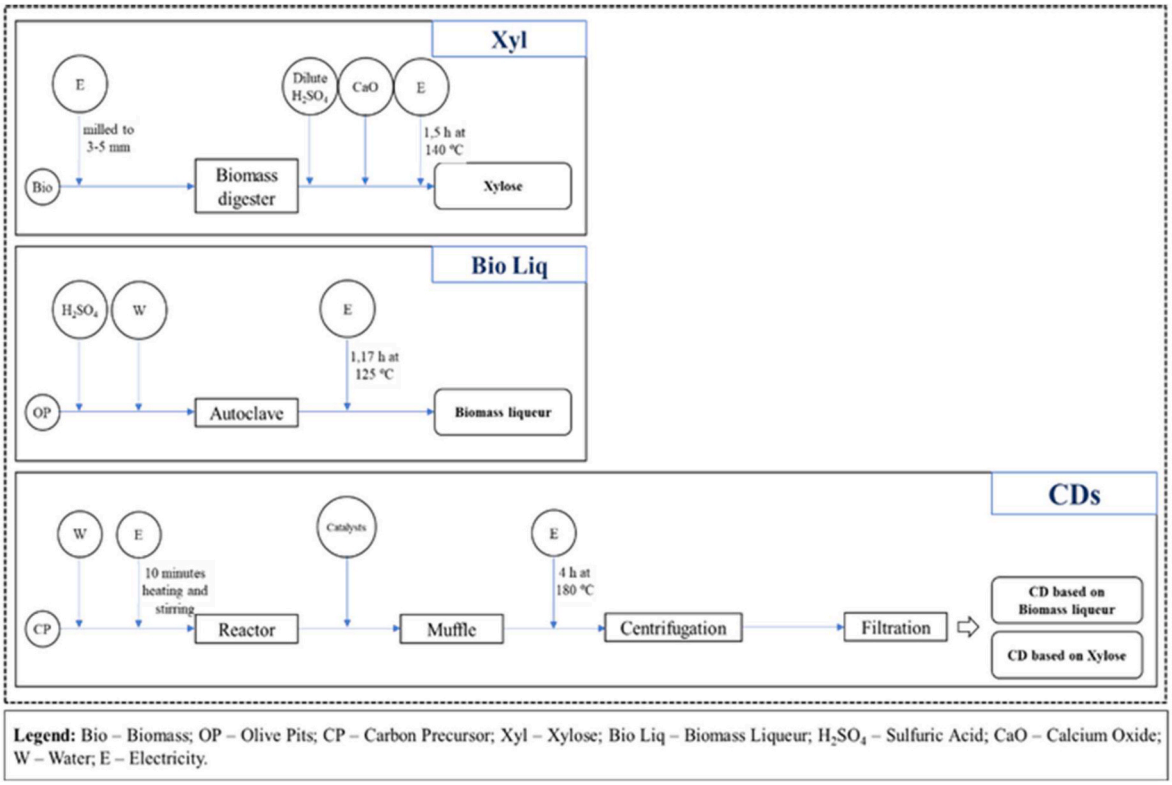

Scheme 2. Diagram for carbon precursors syntheses and CDs synthesis.

Table 2
Data inventory used from Ecoinvent® 3.5 database of raw materials for each CDs under study, in which quantities are referred to 1 kg of CDs. For xylose synthesis/raw materials it was considered the information provided previously (Sharma et al., 2021).

Raw Materials	Ecoinvent® 3.5 database	Amount
Biomass Liqueur		
Sulfuric Acid	Sulfuric acid {RER}	0.03 kg
Water	Water, deionized, from tap water, at user {Europe without Switzerland}	1.48 kg
Electricity	Electricity, medium voltage {ES}	3.82 kWh
Carbon Dots		
Carbon Precursor	Xylose or Biomass Liqueur	1.29 kg
Water	Water, deionized, from tap water, at user {Europe without Switzerland}	17.53 kg
Electricity	Electricity, medium voltage {ES}	7.42 kWh

scenarios (Pianosi et al., 2016), which consist of varying the amount and country origin of the required electricity. More specifically, in a first scenario was considered the variation of the amount of electricity for biomass liqueur. It was also considered a scenario related to the origin of electricity production (Spain, United States (USA) and Brazil (BR)) for both raw materials (xylose and biomass liqueur). This scenario intends to determine how the location of electricity production affects the environmental sustainability of the routes and the raw materials synthesis once each country has a specific energy matrix (Kumar et al., 2021). This analysis is not directly related with countries involved in olive oil industry but is instead with the evaluation of environmental impacts of employing electricity with different and known mixes of renewable/non-renewable energy.

3. Results and discussion

In previous works, we have demonstrated that CDs can be successfully synthesized by using heterogeneous catalysis, thus avoiding the CDs impurification with adatoms (Algarra et al., 2018, 2019; Rodriguez-Padrón et al., 2018). Here, we propose two solid acid catalysts, $VOPO_4{\cdot}2H_2O$ and $NbOPO_4{\times}H_2O$, for synthesizing CDs free of impurities. Afterwards, we will show that the CDs can be functionalized by heteroatoms (N) using those catalysts to modify their optical properties. As previously mentioned, those catalysts were both assayed in a hydrothermal heterogeneous catalysed synthesis of CDs from commercial xylose and biomass liquor.

The presence of CDs in the solution after reaction was confirmed visually through exposure to UV lamp (Figure SI7). The samples that did not show any fluorescence either had no catalyst (blank) or the reaction time was not enough to develop CDs and thus were discarded. Every sample treated with $VOPO_4$ or $NbOPO_4$ showed fluorescence, thus were analyzed by means of TEM. In addition, remaining xylose after reaction was controlled by HPLC for both CDs solutions from biomass and from commercial xylose. Conversion of commercial xylose was estimated at 77.7% ($VOPO_4$) and 65.3% ($NbOPO_4$) and for biomass 86.6% ($VOPO_4$). It must be noted that these conversions do not fully correspond to a real CDs yield, since not all the xylose that is reacting transforms into CDs.

3.1. Morphological analysis

TEM images for commercial xylose derived CDs presented homogeneous quasi spherical nanoparticles whose size range varied from 2 to 6 nm (Fig. 1A and B and Figures SI8A,B), irrespective of the catalyst they were obtained with and if they underwent doping or not. It was observed (Fig. 1B) that a major density of nanoparticles was obtained when working with $VOPO_4$ catalyst, NH_4Cl as dopant and commercial xylose for reaction time of 4 h. While for biomass carbon source, a major concentration was observed when working with $NbOPO_4$ catalyst (Figures SI8C,D). Biomass derived CDs were also notably bigger than the ones synthesized from commercial xylose, presenting an average size of 15 nm. Abundance was strongly affected by the catalyst for biomass liquors. While when performing the synthesis with $NbOPO_4$ a great quantity of CDs was obtained, when switching the catalyst to $VOPO_4$ in the same reaction conditions, a greater dispersion, and less quantity, either working with the absence of dopant (Fig. 1C) or with the presence of it (Fig. 1D). Fig. 2 shows an example of size histograms for commercial xylose N-CDs and biomass liquor N-CDs, due to the difficulty of

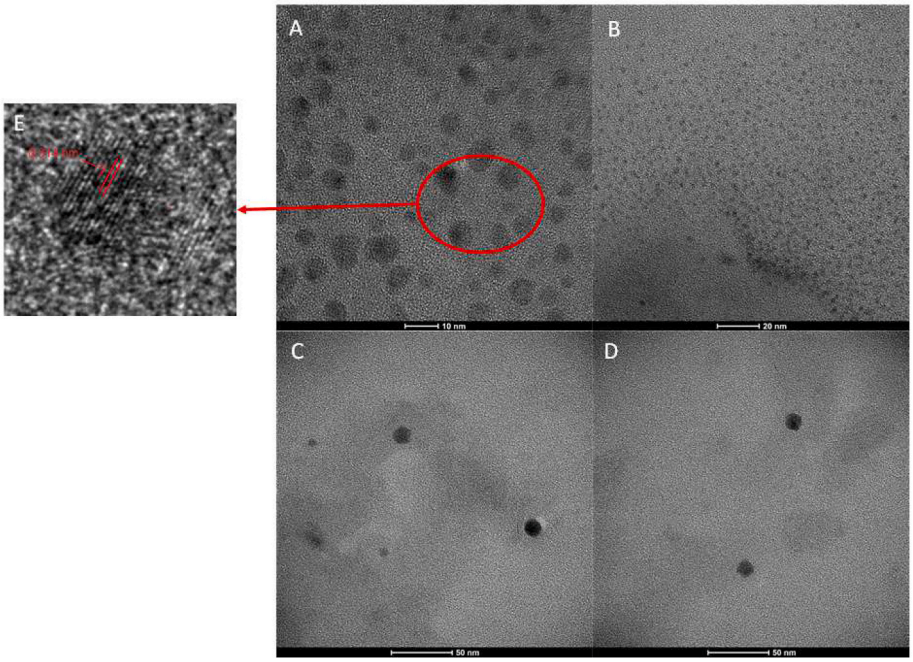

Fig. 1. TEM images of **(A)** Pristine CDs from xylose and $VOPO_4$ catalyst; **(B)** N-CDs from xylose and $VOPO_4$ catalyst; **(C)** CDs from biomass liquor and $VOPO_4$ catalyst; **(D)** N-CDs from biomass liquor and $VOPO_4$ catalyst and **(E)** Graphite spacing in CDs from commercial xylose and $VOPO_4$ catalyst.

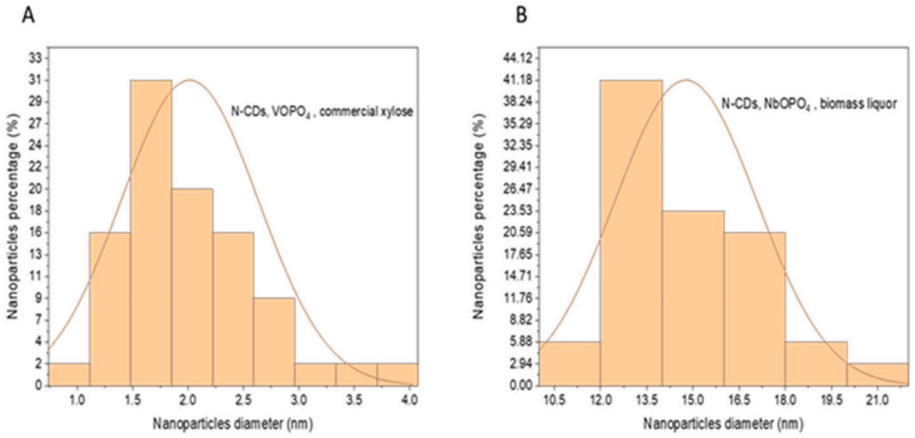

Fig. 2. (**A**) N-CDs from $VOPO_4$ and commercial xylose size histogram and (B) N-CDs from $NbOPO_4$ and biomass liquor size histogram (**B**).

measuring CDs when the outline of each nanoparticle is not completely defined, the size measurements were carried out on commercial xylose N-CDs from $VOPO_4$ catalyst and on biomass liquor N-CDs from $NbOPO_4$ catalyst, since for the rest of cases it was not possible to measure a representative number of nanoparticles for the size histogram. The use of analogue $VOPO_4$ and $NbOPO_4$ catalysts, provided analogue results in the synthesis, in particle size and shape.

Since biomass liquors CDs are full of different oxidation-prone compounds that cannot be separated from the reaction medium, $VOPO_4$ might be acting as a catalyst promotion further oxidation of other organic compounds rather than dehydration of xylose and subsequent aggregation into CDs. For further confirmation of the presence of CDs, the graphitic lattice was identified in HR-TEM images and the measurement of the spacing gave out a value of 0.314 nm (Fig. 1E) (Hembacher et al., 2003; Zheng et al., 2017). Similar found for CDs from xylose and $NbOPO_4$ catalyst (Figure SI8E).

3.2. Surface analysis

After having confirmed, by TEM, the existence of the CDs in the reaction solution, with the aim of confirming the functionalization in the surface of CDs, a XPS analysis was performed in a lyophilized sample of commercial xylose CDs (Fig. 3A). Samples after dialysis were cleaner of organic residues from reaction solution, hence the band that corresponds to C–C binding energy is more intense than those corresponding to –C═O and O–C═O binding energies, as it would be expected from CDs, since are mainly composed of graphitic carbon. The C1*s* core level spectrum obtained was deconvoluted into three mayor contributions (Table 3). The first band (248.8 eV) can be related to simple C–C bond (adventitious carbon), while second and third bands present maximums at 286.6 eV and 288.0 eV, respectively that can be related to carbonyl and carboxylate groups (Patra et al., 2023; Wang et al., 2023).

XPS analysis of commercial xylose N-doped samples confirmed N-doping was successful (Fig. 3B and C). Nitrogen atoms on CDs were

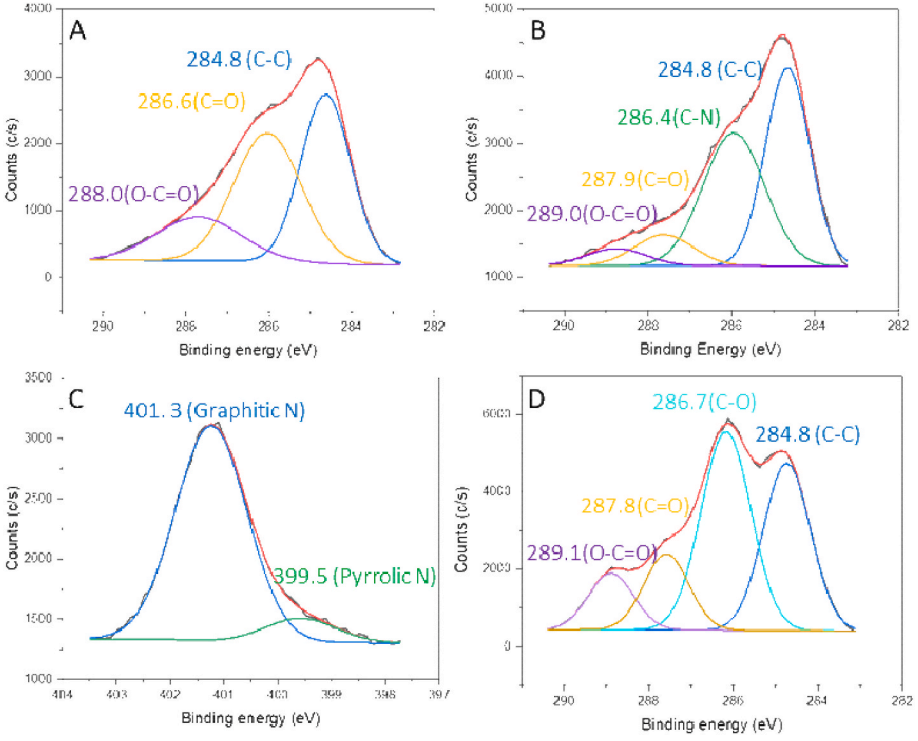

Fig. 3. XPS core level spectra for **(A)** C 1*s* of commercial xylose CDs. **(B)** C 1*s* of commercial xylose N-CDs; **(C)** N 1*s* of commercial xylose N-CDs; **(D)** C 1*s* of biomass liquor CDs.

Table 3
Assignation of the binding energies resulted from the deconvolution of C1*s* core level of CDs synthesized from commercial xylose and biomass liquor and $VOPO_4$ as catalyst.

	C1*s* (eV)	C assignation	N1*s* (eV)	N assignation
Commercial xylose CDs	284.8 (49.27%)	C–C	N/A	
	286.6 (34.54%)	C═O		
	288.0 (16.19%)	O–C═O		
Biomass liquor CDs	284.4 (34.65%)	C–C	N/A[a]	
	286.7 (38.50%)	C–O		
	287.8 (15.25%)	C═O		
	289.1 (11.60%)	O–C═O		
Commercial xylose, N-CDs	284.8 (53.22%)	C–C[		
	286.4 (32.46%)	C–N	401.3 (91.84%)	Graphitic N
	287.9 (8.51%)	C═O	399.5 (8.16%)	Pyrrolic N
	289.0 (5.81%)	O–C═O		

[a] Note: Biomass liquor N-CDs are not presented in this table due to the difficulty observed in obtaining and deconvoluting spectra data from these nanoparticles, since they cannot be totally separated from the rest of components of the reaction media.

mainly found as graphitic nitrogen, but there was also a small amount in the form of pyrrolic nitrogen (Table 3) (Huang et al., 2023). For the C1s core level, it was also possible to confirm the existence of the C–N bond (Table 3). Biomass liquor CDs were also analyzed by means of XPS (Fig. 3D). Obtaining the following deconvoluted spectrum for C 1*s* core level (Table 3). Generally, for CDs, the band for C–C bonding should be the highest band in intensity, due to the graphite carbon core of the CDs, but for biomass liquor, since it has many other substances that are impossible to separate from reaction medium, it can be seen in the XPS a major band for C–O whose contribution can be arose from those substances. Due to the difficulty of obtaining clear XPS spectra for biomass CDs samples in general, for those that were doped, the success of the inclusion of N atoms was confirmed by EDS (Figure SI9). All related survey spectra are presented in Figure SI10.

The survey and the XPS core level of C1s and C1s and the spectra binding energies for CDs from $NbOPO_4$ are also compiled in the SI (Figure SI11-12 and Table SI3). Additional FTIR analysis were carried out for further confirmation of the functional groups decorating the surface of the CDs (Figure SI13).

3.3. Photoluminescence (PL) analysis

PL is considerably higher for the solutions where catalysts were added and for those that were set at 4 h reaction time. A greater amount of PL registered can be related to a greater presence of nanoparticles in the solution, consequently the catalysts, as suspected in TEM, do stimulate the reaction. Similarly, to TEM results, samples where the selected catalyst was $VOPO_4$ exhibited slightly better results. CDs show hugely particular photoluminescence properties, thus are extremely sensitive to irradiation wavelength and its maximum emission peak is highly tuneable. Generally, if irradiated at longer wavelengths using low energy lasers, the maximum undergoes a bathochromic shift, that can be observed for CDs from commercial xylose as well as for biomass CDs (Fig. 4A and B).

Since CDs main applications in bioimaging, sensing and photocatalyst are strongly dependent on their capacity to produce a high amount of photoluminescent emission, it was necessary to perform photoluminescence measurements to confirm whether their photoluminescence emission was as expected and to know their wavelength of emission. Furthermore, since doping the CDs was pursued as a mean to improve the photoluminescence values, these measurements were carried out to corroborate whether the doping met the target. Wavelength emission values for CDs depend on several factors that can be sum up in two main categories: particle size and contributions from different functional groups. Since for the case of CDs coming from commercial xylose a greater homogeneity in size was observed, the bands appearing in the spectra can be related to different groups emitting, rather than to different size particles. These contributions can be explored carrying out a deconvolution of photoluminescence band. It was selected for deconvolution the band corresponding to the sample treated during 4 h with the addition of $VOPO_4$ catalyst (Fig. 4A). Two main contributions appeared on the spectrum, the first one around 500 nm, the second one near 600 nm. The main contribution (500 nm) can be assigned to the emission produced by simple C–O bonds, while the second contribution can be related to the emission of carbonylic groups (-C═O) (van Dam et al., 2017). Therefore, photoluminescence results suggested that the surface of the synthesized CDs might be functionalized by carboxylic acids, and it is possible to confirm that the PL effect is explained by the transitions $n \rightarrow \pi^*$ (Braeuer, 2015; Sun et al., 2018; Chen et al., 2021). The elucidation of the different contributions for the photoluminescence band of biomass CDs is difficult to perform, since not only the number of different groups functionalizing the surface is potentially bigger than for the case of commercial xylose CDs, but due to the greater heterogeneity in size. Although the bathochromic shift observed in biomass CDs band when compared to xylose photoluminescence band can be associated to a bigger size of the nanoparticles.

PL measurements of pristine CDs samples (Fig. 4B–D), as expected, were lower in intensity than those of doped CDs (Fig. 4E and F), since doping CDs generates defects in the surface that are highly emissive spots and since new N–C bonds are created with doping, there is also a contribution in the PL emission that comes from the variety of functional groups generated thanks to doping. Aging the biomass liquor neither improved nor worsened the results obtained from plain liquor (Fig. 4G), intensity values remained over the same units. The $VOPO_4$ catalyst activity after the second and third cycle was controlled by photoluminescence (Fig. 4H). Although with every cycle the spectra decreased in intensity, it remained emitting, indicating the presence of CDs. The catalyst, thus, can be reused at least for three reaction cycles until having to discard it. Similar tendency was observed when $NbOPO_4$ was recovered and reused in subsequent catalytic cycles (Figure SI14). Contrary to what it was expected, for the case of CDs from commercial xylose and $NbOPO_4$ the intensity of photoluminescent emission was lower than for their analogues obtained using $VOPO_4$ as catalyst, despite of the quantity of CDs being just slightly lower. This behaviour can be attributed to the fact that a greater aggregation is observed for the case of CDs from $NbOPO_4$ catalyst and thus, the effect of auto-absorption arouses (Albani, 2004; Gutiérrez et al., 2022). The greater tendency of aggregation of these CDs was further confirmed by ζ potential measurements.

The resulted value was −11.8 and −10.6 mV for $VOPO_4$ and $NbOPO_4$ respectively. When the obtained value result negative tends to imply that the surrounding electron cloud is dense. A high ζ potential, positive or negative, often involves excellent electrostatic stability and null tendency to form aggregates. Highly dispersed nanoparticles frequently present values ranging from −30 mV to 30 mV, while particles considered neutral go from −10 mV to 10 mV (Pudza et al., 2020). As the measured value is certainly near the neutral interval, the synthesized CDs might end up forming aggregate if conserved in solution, although no aggregate have been observed yet. ζ potential is also very sensitive to pH. As acidity increases it gradually acquire a more positive value. Since the pH in this reaction is set between 1 and 3.5, it seems only natural that

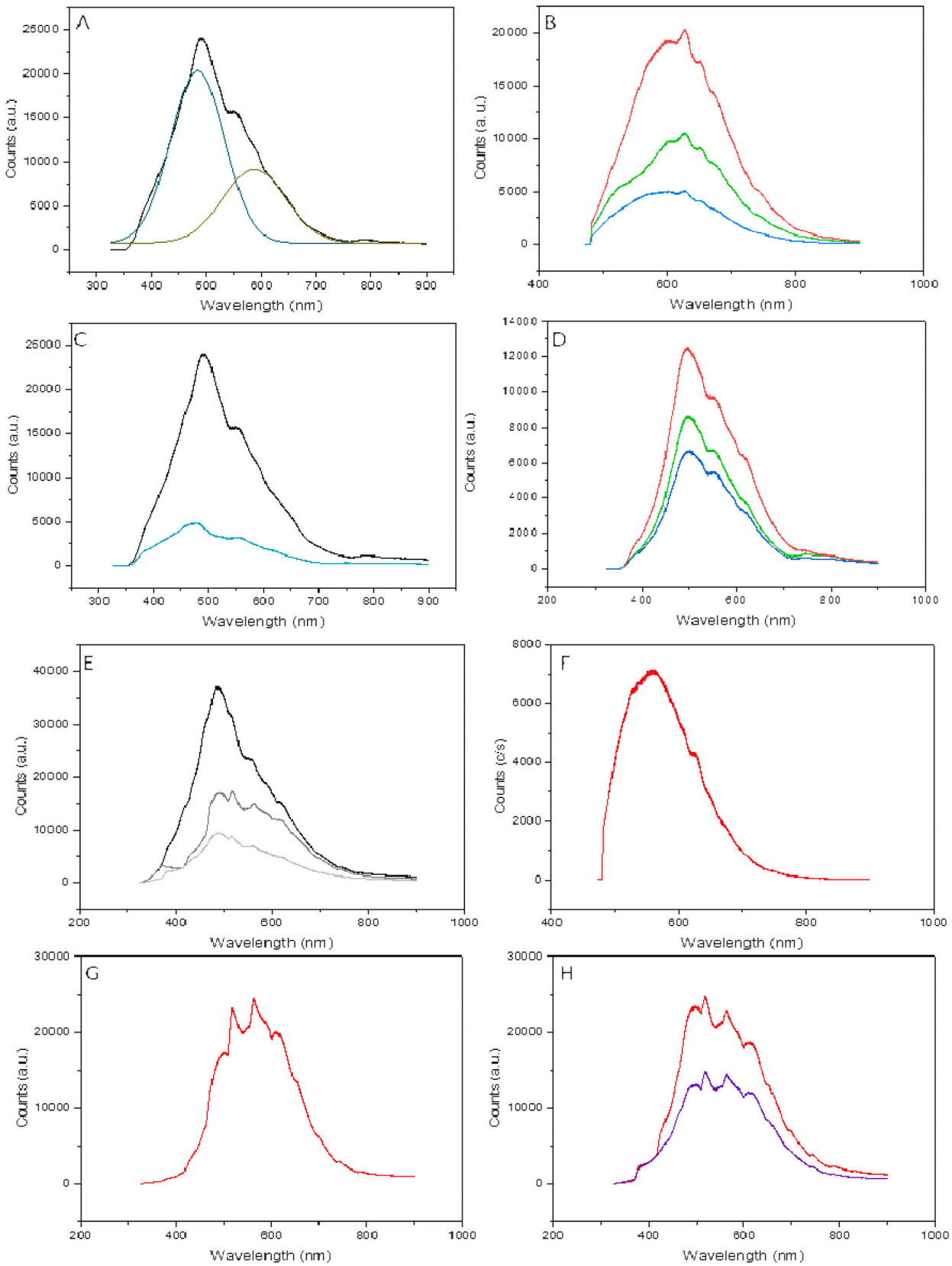

Fig. 4. Photoluminescent emission of **(A)** biomass CDs irradiated with 325 nm excitation laser **(B)** biomass CDs irradiated with 473 nm excitation laser; **(C)** commercial xylose CDs measured with 325 nm excitation laser; **(D)** Deconvolution of the band corresponding to CDs $VOPO_4$, 4 h, 0.75 M xylose, 180 °C; **(E)** N-doped commercial xylose CDs irradiated with 325 nm excitation laser; **(F)** N-doped biomass liquor CDs irradiated with 325 nm excitation laser; **(G)** Aged liquor and **(H)** Recycled $VOPO_4$ catalyst.

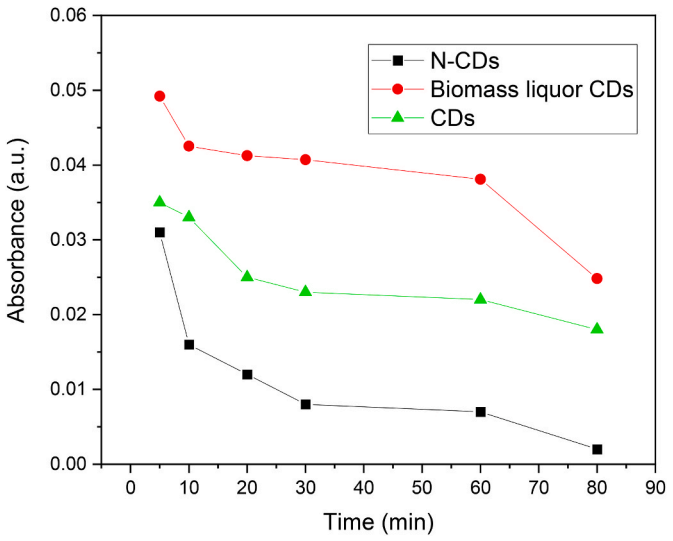

Fig. 5. (**A**) MO degradation catalysed by N-CDs from commercial xylose and VOPO4 as catalyst, pristine CDs from commercial xylose and $VOPO_4$ as catalyst and CDs from biomass liquor and $VOPO_4$ as catalyst.

ζ potential is not extremely negative. When working with biomass derived CDs, however, the quantity of CDs in the sample treated with $NbOPO_4$ as catalyst greatly exceeded the number of CDs present in its analogue sample with $VOPO_4$ as catalyst, but again, the aggregation is such that the auto-absorption effect is incredibly notable, diminishing the intensity of photoluminescence.

3.4. Photocatalytic degradation of methyl orange

The activity of N-doped and pristine CDs in the degradation of methyl orange was compared. N-CDs (Fig. 5A and SI.15A) presented a better yield in contrast to the yield observed for pristine CDs (Fig. 5 and SI.15B). The discoloration was moderate for the case of pristine CDs, while for N-CDs, a faster and more effective degradation was observed. For biomass derived CDs (Figure C), the yield was lower in comparison to CDs from commercial xylose, but still the degradation took place, at a slower rate and lower effectiveness. The differences between commercial CDs and biomass liquor CDs were related to the carbon precursor used that eventually leads to a major or minor formation of CDs, as it was seen in TEM with different qualities that can affect slightly in their performance.

The photocatalytic activity was therefore strongly related to the photoluminescence measurements because the surface state of the CDs is responsible for both their photoluminescent properties and their photocatalytic activity. The final concentration of MO in the solutions after less than 2 h was under the lowest limit of the calibration curved described by 0.1–0.4 ppm standards and it was not possible to determine. The real concentration was then studied by means of TOC.

To perform the TOC analysis and confirm the degradation of methyl orange, an aliquot of reaction medium, that included the presence of N-CDs from commercial source, was analyzed before and after reaction. Moreover, an aliquot of N-CDs to ensure they would not interfere in TOC results was also analyzed without MO. TOC proved that the discoloration observed in UV spectrophotometry was, indeed, a sign of degradation of MO. The analyses showed that the presence of organic compounds diminished after the use of CDs as catalyst for photodegradation and that a solution of CDs provided no signal in TOC, thus it did not interfere in the result of analysis. The TOC results showed (Table 4) that the carbon was reduced up to 99%. These results demonstrated the great photocatalytic activity of the CDs and their potential use in degradation of dyes. The final concentration of MO present (Table 4) in the solution after reaction can be related to what was obtained as final concentration in the study of discoloration in Spectrophotometry UV, having into accounts the limitations in the detection limits.

Table 4
Methyl orange (MO) final concentration obtained from TOC determination.

Samples	MO concentration (ppm)
MO	4.34
N-CDs	0
MO + N-CDs before reaction	4.29
MO + N-CDs after reaction	0.0443

Furthermore, the results of TOC analysis confirmed that no adsorption of MO was detected in dark conditions, as in MO + CDs before reaction sample no alteration of the concentration was observed.

Based on the photocatalytic results, the photodegradation mechanism of MO is portrayed in Scheme 3, where CDs would act as photocatalysts and electron donors, as the carboxylic groups would enhance electron movement, while graphitic N would provide the electrons as the donors. Molecular oxygen is proposed as the acceptor and would then attack methyl orange, causing its degradation (Park et al., 2019; Zhao et al., 2019; Rajapandi et al., 2022).

3.5. LCA results

The comparison of potential environmental impacts between the syntheses under study was made by considering a weight-based functional unit of 1 kg of CDs (Fig. 6) (Crista et al., 2020; Crista, Esteves da Silva and Pinto da Silva 2020; Fernandes, Esteves da Silva and Pinto da Silva, 2021; Chritié, Esteves da Silva and Pinto da Silva 2020). Our objective is to compare the relative contributions of the input materials/energy involved in each synthesis for the different impact categories. Thus, we will not make quantitative appreciations of the environmental impacts. For both syntheses, electricity represents more than 68% of the potential environmental impacts in different categories, which identifies it as a main hotspot in both processes. On the other hand, the relative contributions of deionized water appear to be negligible in the two analyzed processes. The contributions of carbon precursor to the different impact categories (in both syntheses) are not negligible but appear to be significantly less relevant than that of electricity.

Comparing both syntheses, the immediate conclusion is that the CDs produced from xylose are associated with lower environmental impacts in all categories. This does not mean, however, that CDs from biomass liqueur should not be further explored. For the contrary, this LCA should be used to investigate why higher environmental impacts results from CDs Biomass Liqueur, in these conditions, so that we can address it and reduce the associated impacts. This should be pursued so that biomass waste can be properly valorised as a raw material.

While electricity is the main hotspot in both syntheses, its consumption is the same in both processes, and so, it cannot be the reason for the different relative environmental impacts (Table 2).

More specifically, the differences should be attributed to the carbon precursor (which is the different parameter between the syntheses). In fact, xylose in CDs Xylose contributes 12% for Human Health impacts, 13% for Ecosystems and 14% for the Resources category, while in CDs Biomass Liqueur the carbon precursor represents about 31% in both Human Health, Ecosystems and Resources. So, the carbon precursor appears to be a key parameter to determine the sustainability of these CDs syntheses. This finding is in line with previous LCA of fabrication routes for CDs (Fernandes, Esteves da Silva and Pinto da Silva, 2020; Sendão et al., 2020). Given this, reducing the environmental impacts associated with the production of the carbon precursor should the focus for increasing the environmental sustainability of CD Biomass Liqueur. To better understand how this can be achieved, the relative environmental impacts for the synthesis of xylose synthesis are shown in Fig. 7A, while the results obtained to produce biomass liqueur are found on

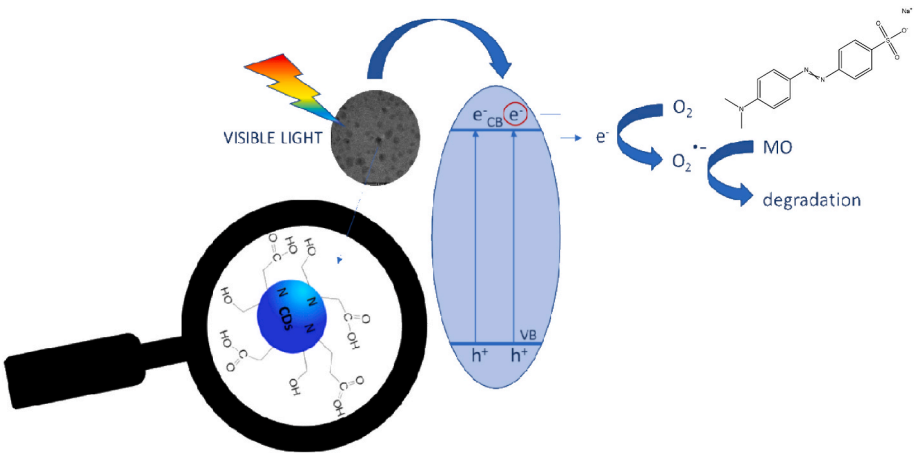

Scheme 3. Photocatalytic mechanism of MO degradation.

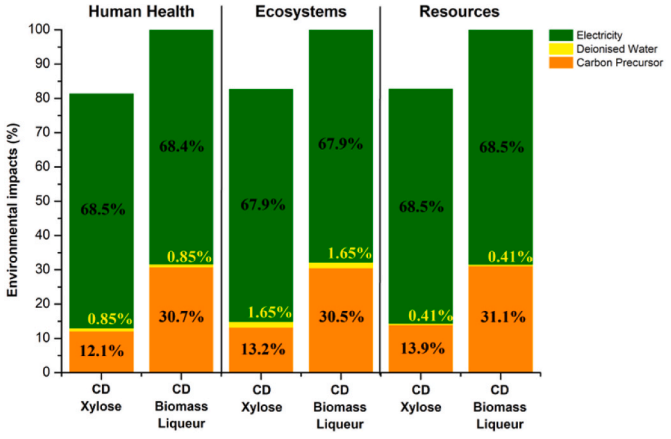

Fig. 6. Relative environmental impacts of both syntheses (CDs Xylose and CDs Biomass Liqueur). This graphic was obtained applying ReCiPe endpoint method.

Fig. 7B. According to Fig. 7A, the major contributor to the environmental impacts generated by xylose synthesis is electricity, as it presents contributions between 78% and 89%. Deionized water, sulfuric acid, and calcium oxide have a negligible influence on the associated potential environmental impacts. However, sugarcane represents about 9% in Ecosystem category and steam is responsible for approximately 20% of environmental impacts in Resources category.

On the other hand, the production of biomass liqueur appears to have only one parameter responsible for relevant environmental impacts, since electricity is responsible for about 98% contributions for the Resources category and 99% contribution for both Human Health and Ecosystems associated impacts. Thus, electricity appears to be the main hotspot in the synthesis of both carbon precursors, with higher relative contributions to produce biomass liqueur.

Given this, electricity should be the parameter to be focused on to reduce the environmental impacts associated with the production of biomass liqueur, and consequently of CDs Biomass Liqueur. In fact, we have used here data obtained at the laboratory-scale, in which the consumption of electricity from used equipment might not be the most efficiently scaled with the amount of generated materials. Therefore, optimization of the consumption of electricity should lead to lower environmental impacts associated with this process. To showcase this possibility, we performed a sensitivity analysis in which we varied the amount of consumed electricity (reduction of 2, 3 and 6 times the normal amount). Interestingly, the decrease of the amount of electricity in the production of biomass liqueur did lead to lower impacts than the synthesis of xylose. More specifically, the production of biomass liqueur would be more sustainable than the synthesis of xylose if the amount of used electricity was at least three times lower than the amount effectively used. To further understand the influence of electricity on the production of biomass liqueur we also performed a sensibility analysis, in which we varied the amount of used electricity (Figure SI16)

Considering this, it was performed an analysis to evaluate the differences between three countries regarding electricity production (Fig. 8). This analysis showed that for both carbon precursors, there is a

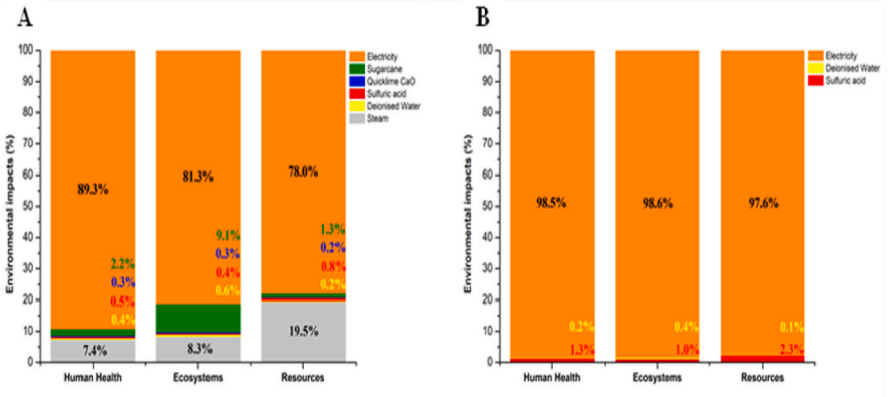

Fig. 7. (**A**) Relative environmental impacts of xylose. This graphic was obtained applying ReCiPe endpoint method. **(B)** Relative environmental impacts of biomass liqueur. This graphic was obtained applying ReCiPe endpoint method.

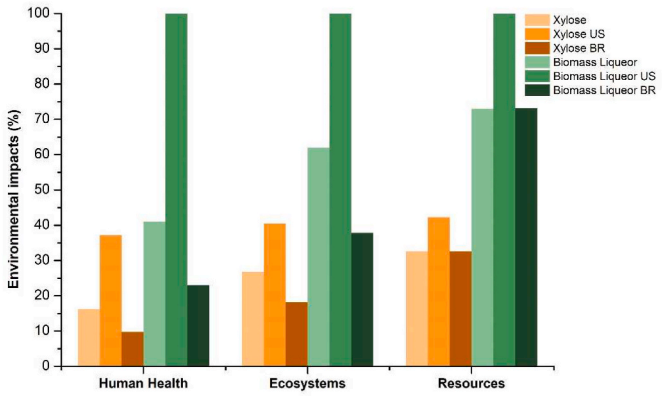

Fig. 8. Relative environmental impacts for sensibility analysis of both carbon precursors syntheses (xylose and biomass liqueur), considering electricity production from different countries. ES refers to Spain, US refers to United States and BR refers to Brazil. This graphic was obtained applying ReCiPe endpoint method.

trend regarding the electricity production in different countries (Brazil < Spain < USA).

That agrees with a study carried out by Ecoinvent database, in which was discovered that the impacts associated with energy production were smaller in all countries in the European Community than the impacts for scenarios for the US. This is justified because the energy matrix in the US is basically based on coal and natural gas, while in Europe the energy production is also reliant on coal, but many countries also have relevant sources of renewable energy. On the other hand, the impacts associated with energy production in Brazil were smaller because the energy matrix is basically composed of clean and renewable energy sources, such as hydroelectric dams (Zhao et al., 2019).

4. Conclusions

The capacity of both catalysts $VOPO_4$ and $NbOPO_4$ of promoting the synthesis of carbon nanoparticles have been proved, being optimal for $VOPO_4$ according to results obtained for xylose conversion, photoluminescence and TEM that indicated a greater quantity of nanoparticles present in the solution. Reaction time was also a determinant factor in the synthesis of CDs, being 4 h the one that showed to be the most fruitful. Nanoparticles' synthesis was feasible from commercial carbon precursor as well as from biomass precursor. The slight differences in results established between both carbon sources were almost certainly due to the concentration and composition difference. The synthesized nanoparticles stand out for their size homogeneity. Surface characterization proved that the synthesized CDs are functionalized by carboxylate groups that caused the emission observed when irradiated with UV. ζ potential analysis suggested a tendency to form aggregates, although in TEM images no aggregates were spotted, on the contrary, a great dispersion was observed, thus permitting the identification of graphitic lattice and the measurement of its spacing. Doped CDs, especially, N-doped CDs showed great potential in photoluminescent applications, since their emissive values exceeded greatly those obtained from pristine CDs. To check the photoactivity of the obtained CDs from xylose was tested in the photocatalytic degradation of methyl orange as probe and showed promising results, demonstrated that is possible the valorisation for further process of catalyst. A LCA was also performed to understand the environmental impacts associated with each synthesis route here studied. This was achieved by considering both the synthesis of CDs and the carbon precursor production. We have found that while electricity was found to be a major contributor to all categories for synthesis, the parameter that explain the differences in sustainability between these processes is the identity of the carbonous precursor. Following this, we have further analysis the sustainability of the production of each carbon precursor (xylose and biomass liqueur). This showed that electricity is a main hotspot in the current process to produce biomass liqueur.

Ethics approval and consent to participate

Not applicable.

Consent for publication

Not applicable.

CRediT authorship contribution statement

Gabriela Rodríguez-Carballo: Conceptualization, Formal analysis, Writing – original draft, Writing – review & editing, Methodology, Resources, Formal analysis, Writing – review & editing, Formal analysis, Writing – review & editing, Conceptualization, Resources, Formal analysis. **Ramón Moreno-Tost:** Conceptualization, Formal analysis, Writing – original draft, Writing – review & editing. **Sónia Fernandes:** Methodology, Resources, Formal analysis, Writing – review & editing, Formal analysis, Writing – review & editing, Conceptualization, Resources, Formal analysis. **Joaquim C.G. Esteves da Silva:** Methodology, Resources, Formal analysis, Writing – review & editing, Formal analysis, Writing – review & editing, Conceptualization, Resources, Formal analysis. **Luís Pinto da Silva:** Conceptualization, Formal analysis, Writing – original draft, Writing – review & editing. **Eulogio Castro Galiano:** Methodology, Resources, Formal analysis, Writing – review & editing, Formal analysis, Writing – review & editing, Conceptualization, Resources, Formal analysis. **Manuel Algarra:** Conceptualization, Formal analysis, Writing – original draft, Writing – review & editing.

Declaration of competing interest

The authors declare that they have no known competing financial interests or personal relationships that could have appeared to influence the work reported in this paper.

Data availability

No data was used for the research described in the article.

Acknowledgments

This research was funded by the Spanish Ministry of Science and Innovation (PID2021- 122736OB-C42), FEDER (European Union) funds (PID2021-122736OB-C42, P20-00375, UMA20- FEDERJA88). M.A thanks to the Spanish Ministry of Science and Innovation (MCIN/AEI/10.13039/501100011033) through project PID2021-122613OB-I00. This work was made in the framework of projects UIDB/00081/2020 (CIQUP), UIDB/05748/2020 (GreenUPorto), LA/P/00081/2020 (IMS), and PTDC/QUI-QFI/2870/2020, funded by the Portuguese Foundation for Science and Technology (FCT, Lisbon). Luís Pinto da Silva acknowledges funding from FCT under the Scientific Employment Stimulus (CEECINST/00069/2021), while S.F acknowledges FCT for funding of her Ph.D. grant (2021. 05479.BD). The Laboratory of Computational Modelling of Environmental Pollutants-Human Interactions (LACOMEPHI) is acknowledged.

Appendix A. Supplementary data

Supplementary data to this article can be found online at https://doi.org/10.1016/j.jclepro.2023.138728.

References

Afonso, A.C.P., Correia, A.S., Duarte, D., Brandão, A.T.S.C., Martínez de Yuso, M.V., Jiménez- Jiménez, J., Vale, N., Pereira, C.M., Algarra, M., Pinto da Silva, L., 2021. An active surface preservation strategy for the rational development of carbon dots as pH-responsive fluorescent nanosensors. Chemosensors 9, 191. https://doi.org/10.3390/chemosensors9080191.

Albani, J.R., 2004. Fluorescence: Principles and Observables, en: Structure and Dynamics of Macromolecules: Absorption and Fluorescence Studies. Elsevier, pp. 55–98, 2004.

Algarra, M., González-Calabuig, A., Radotić, K., Mutavdzic, D., Ania, C.O., Lázaro-Martínez, J.M., Jiménez-Jiménez, J., Rodríguez-Castellón, E., del Valle, M., 2018. Enhanced electrochemical response of carbon quantum dot modified electrodes. Talanta 178, 679–685. https://doi.org/10.1016/j.talanta.2017.09.082.

Algarra, M., dos Orfãos, L., Alves, C.S., Moreno-Tost, R., Pino-González, M.S., Jiménez-Jiménez, J., Rodríguez-Castellón, E., Eliche-Quesada, D., Castro, E., Luque, R., 2019. Sustainable production of carbon nanoparticles from Olive pit biomass: understanding proton transfer in the excited state on carbon dots. ACS Sustain. Chem. Eng. 7, 10493–10500. https://doi.org/10.1021/acssuschemeng.9b00969.

Braeuer, A., 2015. Interaction of matter and electromagnetic radiation, en: In situ Spectroscopic Techniques at High Pressure. Elsevier, pp. 41–192.

Bramhaiah, K., Bhuyan, R., Mandal, S., Kar, S., Prabhu, R., John, N.S., Gramlich, M., Urban, A.S., Bhattacharyya, S., 2021. Molecular, aromatic, and amorphous domains of N-carbon dots: leading toward the competitive photoluminescence and photocatalytic properties. J. Phys. Chem. C Nanomater. Interfaces. 125, 4299–4309. https://doi.org/10.1021/acs.jpcc.1c00004.

Campos, B.B., Contreras-Cáceres, R., Bandosz, T.J., Jiménez-Jiménez, J., Rodríguez-Castellón, E., Esteves da Silva, J.C.G., Algarra, M., 2016. Carbon dots as fluorescent sensor for detection of explosive nitrocompounds. Carbon 106, 171–178. https://doi.org/10.1016/j.carbon.2016.05.030.

Chen, X., Wu, W., Zhang, W., Wang, Z., Fu, Z., Zhou, L., Yi, Z., Li, G., Zeng, L., 2021. Blue and green double band luminescent carbon quantum dots: synthesis, origin of photoluminescence, and application in white light-emitting devices. Appl. Phys. Lett. 118, 153102 https://doi.org/10.1063/5.0046495.

Christé, S., Esteves da Silva, J.C.G., Pinto da Silva, L., 2020. Evaluation of the environmental impact and efficiency of N-doping strategies in the synthesis of carbon dots. Materials 13, 504. https://doi.org/10.3390/ma13030504.

El-Shabasy, R.M., Farouk Elsadek, M., Mohamed Ahmed, B., Fawzy Farahat, M., Mosleh, K.N., Taher, M.M., 2021. Recent developments in carbon quantum dots: properties, fabrication techniques, and bio-applications. Processes 9, 388. https://doi.org/10.3390/pr9020388.

Fernandes, S., Esteves da Silva, J.C.G., Pinto da Silva, L., 2020. Life Cycle Assessment of the sustainability of enhancing the photodegradation activity of TiO_2 with metal-doping. Materials 13, 1487. https://doi.org/10.3390/ma13071487.

Fernandes, S., Esteves da Silva, J.C.G., Pinto da Silva, L., 2021. Comparative life cycle assessment of high-yield synthesis routes for carbon dots. NanoImpact 23, 100332. https://doi.org/10.1016/j.impact.2021.100332.

Gutiérrez, M., Zhang, Y., Tan, J.C., 2022. Confinement of luminescent guests in metal-organic frameworks: understanding pathways from synthesis and multimodal characterization to potential applications of LG@MOF systems. Chem. Rev. 122, 10438–10483. https://doi.org/10.1021/acs.chemrev.1c00980.

Hao, Q., Qiao, L., Shi, G., He, Y., Cui, Z., Fu, P., Liu, M., Qiao, X., Pang, X., 2021. Effect of nitrogen type on carbon dot photocatalysts for visible-light-induced atom transfer radical polymerization. Polym. Chem. 12, 3060–3066. https://doi.org/10.1039/d1py00148e.

Hembacher, S., Giessibl, F.J., Mannhart, J., Quate, C.F., 2003. Revealing the hidden atom in graphite by low-temperature atomic force microscopy. Proc. Natl. Acad. Sci. USA 100, 12539–12542. https://doi.org/10.1073/pnas.2134173100.

Hola, K., Zhang, Y., Wang, Y., Giannelis, E.P., Zboril, R., Rogach, A.L., 2014. Carbon dots- Emerging light emitters for bioimaging, cancer therapy and optoelectronics. Nano Today 9, 590–603. https://doi.org/10.1016/j.nantod.2014.09.004.

Huang, H., Shi, M., Zhai, H., Zhang, Y., Zhang, Y., Zhao, Y., 2023. Nitrogen-doped carbon dots as visible light initiators for 3D (Bio)Printing. Polym. Chem. 14, 268–276. https://doi.org/10.1039/d2py01324j.

Huijbregts, M.A.J., Steinmann, Z.J.N., Elshout, P.M.F., Stam, G., Verones, F., Vieira, M., M. Zijp, M., Hollander, A., van Zelm, R., 2017. ReCiPe2016: a harmonised life cycle impact assessment method at midpoint and endpoint level. Int. J. Life Cycle Assess. 22, 138–147. https://doi.org/10.1007/s11367-016-1246-y.

Jung, H., Sapner, V.S., Adhikari, A., Sathe, B.R., Patel, R., 2022. Recent progress on carbon quantum dots based photocatalysis. Front. Chem. 10, 881495 https://doi.org/10.3389/fchem.2022.881495.

Kaur, A., Gupta, U., Hasan, I., Muhammad, R., Ahmad Khan, R., 2021. Synthesis of highly fluorescent carbon dots from spices for determination of sunset yellow in beverages. Microchem. J. 170, 106720 https://doi.org/10.1016/j.microc.2021.106720.

Khan, M.E., Mohammad, A., Yoon, T., 2022. State-of-the-art developments in carbon quantum dots (CQDs): photo-catalysis, bio-imaging, and bio-sensing applications. Chemosphere 302, 134815. https://doi.org/10.1016/j.chemosphere.2022.134815.

Kumar, M., Choubey, V.K., Deepak, A., Gedam, V.V., Raut, R.D., 2021. Life cycle assessment (LCA) of dairy processing industry: a case study of North India. J. Clean. Prod. 326, 129331 https://doi.org/10.1016/j.jclepro.2021.129331.

Kurian, M., Paul, A., 2021. Recent trends in the use of green sources for carbon dot synthesis - a short review. Carbon Trends 3, 100032. https://doi.org/10.1016/j.cartre.2021.100032.

Li, J., Zuo, G., Qi, X., Wei, W., Pan, X., Su, T., Zhang, J., Dong, W., 2017. Selective determination of Ag^+ using Salecan derived nitrogen doped carbon dots as a fluorescent probe. J. Mater. Sci. Eng. C 77, 508–512. https://doi.org/10.1016/j.msec.2017.04.007.

Li, J., Zuo, G., Pan, X., Wei, W., Qi, X., Su, T., Don, W., 2018. Nitrogen-doped carbon dots as a fluorescent probe for the highly sensitive detection of Ag^+ and cell imaging. Luminescence 33, 243–248. https://doi.org/10.1002/bio.4236.

Luo, Z., Liu, E., Hu, T., Li, Z., Liu, T., 2015. Effect of synthetic methods on electrochemical performances of $VOPO_4{\cdot}2H_2O$ supercapacitor. Ionics 21, 289–294. https://doi.org/10.1007/s11581-014-1317-7.

Macairan, J.R., de Medeiros, T.V., Gazzetto, M., Yarur Villanueva, F., Cannizzo, A., Naccache, R., 2022. Elucidating the mechanism of dual-fluorescence in carbon dots. J. Colloid Interface Sci. 606, 67–76. https://doi.org/10.1016/j.jcis.2021.07.156.

Marras, Masia, S., Duce, P., Spano, D., Sirca, C., 2015. Carbon footprint assessment on a mature vineyard. Agric. For. Meteorol. 214–215, 350–356. https://doi.org/10.1016/j.agrformet.2015.08.270.

Nocito, G., Calabrese, G., Forte, S., Petralia, S., Puglisi, C., Campolo, M., Esposito, E., Conoci, S., 2021. Carbon Dots as promising tools for cancer diagnosis and therapy. Cancers 13, 1991. https://doi.org/10.3390/cancers13091991.

Park, C.H., Hira, S.A., Muthuchamy, N., Park, S., Park, K.H., 2019. Synthesis of silver nanostructures in ionic liquid media and their application to photodegradation of methyl orange. Nanomater. Nanotechnol. 9, 184798041983650 https://doi.org/10.1177/1847980419836500.

Patra, S., Singh, M., Subudhi, S., Mandal, M., Nayak, A.K., Sahu, B.B., Mahanandia, P., 2023. One-step green synthesis of in–situ functionalized carbon quantum dots from Tagetes patula flowers: applications as a fluorescent probe for detecting Fe^{3+} ions and as an antifungal agent. J. Photochem. Photobiol. Chem. 442, 114779 https://doi.org/10.1016/j.jphotochem.2023.114779.

Perikala, M., Bhardwaj, A., 2021. Excellent color rendering index single system white light emitting carbon dots for next generation lighting devices. Sci. Rep. 11, 11594 https://doi.org/10.1038/s41598-021-91074-w.

Pianosi, F., Beven, K., Freer, J., Hall, J.W., Rougier, J., Stephenson, D.B., Wagener, T., 2016. Sensitivity analysis of environmental models: a systematic review with practical workflow. Environ. Model. Software 79, 214–232. https://doi.org/10.1016/j.envsoft.2016.02.008.

Pudza, M.Y., Zainal Abidin, Z., Abdul Rashid, S., Yasin, F.M., Noor, A.S.M., Issa, M.A., 2020. Eco-friendly sustainable fluorescent carbon dots for the adsorption of heavy metal ions in aqueous environment. Nanomaterials 10, 315. https://doi.org/10.3390/nano10020315.

Rajapandi, S., Pandeeswaran, M., Kousalya, G.N., 2022. Novel green synthesis of N-doped carbon dots from fruits of opuntia Ficus indica as an effective catalyst for the photocatalytic degradation of methyl orange dye and antibacterial studies. Inorg. Chem. Commun. 146, 110041 https://doi.org/10.1016/j.inoche.2022.110041.

Rodríguez-Padrón, D., Algarra, M., Tarelho, L.A.C., Frade, J., Franco, A., de Miguel, G., Jiménez, J., Rodríguez-Castellón, E., Luque, R., 2018. Catalyzed microwave-assisted preparation of carbon quantum dots from lignocellulosic residues. ACS Sustain. Chem. Eng. 6, 7200–7205. https://doi.org/10.1021/acssuschemeng.7b03848.

Sendão, R., Martínez de Yuso, M.V., Algarra, M., Esteves da Silva, J.C.G., Pinto da Silva, L., 2020. Comparative life cycle assessment of bottom-up synthesis routes for carbon dots derived from citric acid and urea. J. Clean. Prod. 254, 120080 https://doi.org/10.1016/j.jclepro.2020.120080.

Sharma, T., Dasgupta, D., Singh, J., Bhaskar, T., Ghosh, D., 2020. Yeast lipid-based biofuels and oleochemicals from lignocellulosic biomass: life cycle impact assessment, Sustain. Energy Fuels 4, 387–398. https://doi.org/10.1039/c9se00540d.

Sharma, S., Saini, S., Khangembam, M., Singh, V., 2021. Nanomaterials-based biosensors for COVID-19 detection-A review. IEEE Sensor. J. 21, 5598–5611. https://doi.org/10.1109/jsen.2020.3036748.

Sim, L.C., Tai, J.Y., Khor, J.M., Wong, J.L., Lee, J.Y., Leong, K.H., Saravanan, P., Aziz, A. A., 2019. Carbon dots synthesized from green precursors with an amplified photoluminescence: Synthesis, characterization, and its application, en: Plant Nanobionics. Springer International Publishing, Cham, pp. 1–33.

Singh, P., Rani, N., Kumar, S., Kumar, P., Mohan, B., Pallavi, Bhankar, V., Kataria, N., Kumar, R., Kumar, K., 2023. Assessing the biomass-based carbon dots and their composites for photocatalytic treatment of wastewater. J. Clean. Prod. 413, 137474 https://doi.org/10.1016/j.jclepro.2023.137474.

Sun, Z., Li, X., Wu, Y., Wei, C., Zeng, H., 2018. Origin of green luminescence in carbon quantum dots: specific emission bands originate from oxidized carbon groups. New J. Chem. 42, 4603–4611. https://doi.org/10.1039/c7nj04562j.

Tajik, S., Dourandish, Z., Zhang, K., Beitollahi, H., Van Le, Q., Jang, H.W., Shokouhimehr, M., 2020. Carbon and graphene quantum dots: a review on syntheses, characterization, biological and sensing applications for neurotransmitter determination. RSC Adv. 10, 15406–15429. https://doi.org/10.1039/d0ra00799d.

Van Dam, B., Nie, H., Ju, B., Marino, E., Paulusse, J.M.J., Schall, P., Li, M., Dohnalová, K., 2017. Excitation-dependent photoluminescence from single-carbon dots. Small 13, 1702098. https://doi.org/10.1002/smll.201702098.

Wang, X., Wang, Y., Pan, W., Wang, J., Sun, X., 2021. Carbon-dot-based probe designed to detect intracellular pH in fungal cells for building its relationship with intracellular polysaccharide. ACS Sustain. Chem. Eng. 9, 3718–3726. https://doi.org/10.1021/acssuschemeng.0c08160.

Wang, Y., Wu, R., Zhang, Y., Cheng, S., Zhang, Y., 2023. High quantum yield nitrogen doped carbon dots for Ag^+ sensing and bioimaging. J. Mol. Struct. 1283, 135212 https://doi.org/10.1016/j.molstruc.2023.135212.

Wu, Y., Li, Y., Pan, X., Hu, C., Zhuang, J., Zhang, X., Lei, B., Liu, Y., 2021. Hemicellulose triggered high-yield synthesis of carbon dots from biomass. New J. Chem. 45, 5484–5490. https://doi.org/10.1039/d1nj00340b.

Wu, Q., Cao, J., Wang, X., Liu, Y., Zhao, Y., Wang, H., Liu, Y., Huang, H., Liao, F., Shao, M., Kang, Z., 2021. A metal-free photocatalyst for highly efficient hydrogen

peroxide photoproduction in real seawater. Nat. Commun. 12, 483. https://doi.org/10.1038/s41467-020-20823-8.

Xiong, H.F., An, B.L., Zhang, J.M., Yin, C.L., Wang, X.H., Wang, J.H., Xu, J.Q., 2021. Efficient one step synthesis of green carbon quantum dots catalyzed by tin oxide, Mater. Today Commun 26, 101762. https://doi.org/10.1016/j.mtcomm.2020.101762.

Yin, C.L., An, B.L., Li, J., Wang, X.H., Zhang, J.M., Xu, J.Q., 2021. High-efficient synthesis of bright yellow carbon quantum dots catalyzed by SnO_2 NPs. J. Lumin. 233, 117850 https://doi.org/10.1016/j.jlumin.2020.117850.

Zhao, B., Wang, B., Lu, H., Dai, S., Huang, Z., 2019. Tuning the visible-light photocatalytic degradation activity of thin nanosheets constructed porous g-C_3N_4 microspheres by decorating ionic liquid modified carbon dots: roles of heterojunctions and surface charges. New J. Chem. 43, 10141–10150. https://doi.org/10.1039/c9nj00308h.

Zheng, B., Chen, Y., Li, P., Wang, Z., Cao, B., Qi, F., Liu, J., Qiu, Z., Zhang, W., 2017. Ultrafast ammonia-driven, microwave-assisted synthesis of nitrogen-doped graphene quantum dots and their optical properties. Nanophotonics 6, 259–267. https://doi.org/10.1515/nanoph-2016-0102.

Zheng, S., Qin, F., Hu, C., Zhang, C., Ma, Y., Yang, R., Wei, L., Bao, L., 2021. Up-converted nitrogen-doped carbon quantum dots to accelerate charge transfer of dibismuth tetraoxide for enhanced full-spectrum photocatalytic activity. Colloids Surf. A Physicochem. Eng. Asp. 615, 126217 https://doi.org/10.1016/j.colsurfa.2021.126217.

Zhu, S., Song, Y., Zhao, X., Shao, J., Zhang, J., Yang, B., 2015. The photoluminescence mechanism in carbon dots (graphene quantum dots, carbon nanodots, and polymer dots): current state and future perspective. Nano Res. 8, 355–381. https://doi.org/10.1007/s12274-014-0644-3.

Zhu, L., Shen, D., Wu, C., Gu, S., 2020. State-of-the-art on the preparation, modification, and application of biomass-derived carbon quantum dots. Ind. Eng. Chem. Res. 59, 22017–22039. https://doi.org/10.1021/acs.iecr.0c04760.

Zhu, Z., Li, X., Luo, M., Chen, M., Chen, W., Yang, P., Zhou, X., 2022. Synthesis of carbon dots with high photocatalytic reactivity by tailoring heteroatom doping. J. Colloid Interface Sci. 605, 330–341. https://doi.org/10.1016/j.jcis.2021.07.016.